AIP | Applied Physics Letters

High performance thin quantum barrier InGaN/GaN solar cells on sapphire and bulk (0001) GaN substrates

N. G. Young, R. M. Farrell, Y. L. Hu, Y. Terao, M. Iza, S. Keller, S. P. DenBaars, S. Nakamura, and J. S. Speck

Citation: Applied Physics Letters **103**, 173903 (2013); doi: 10.1063/1.4826483
View online: http://dx.doi.org/10.1063/1.4826483
View Table of Contents: http://scitation.aip.org/content/aip/journal/apl/103/17?ver=pdfcov
Published by the AIP Publishing

High performance thin quantum barrier InGaN/GaN solar cells on sapphire and bulk (0001) GaN substrates

N. G. Young,[1,a)] R. M. Farrell,[1] Y. L. Hu,[1] Y. Terao,[1,2] M. Iza,[1] S. Keller,[3] S. P. DenBaars,[1,3] S. Nakamura,[1,3] and J. S. Speck[1]
[1]*Materials Department, University of California, Santa Barbara, California 93106, USA*
[2]*Fuji Electric Corp. of America, 100 Century Center Ct., Ste 100, San Jose, California 95112, USA*
[3]*Department of Electrical and Computer Engineering, University of California, Santa Barbara, California 93106, USA*

(Received 16 August 2013; accepted 6 October 2013; published online 22 October 2013)

We demonstrate high performance InGaN/GaN multiple quantum well solar cells with thin quantum barriers and spectral response extending to 460 nm. Devices grown on bulk (0001) GaN substrates with up to 50 quantum wells (QWs) outperform those grown simultaneously on sapphire due to the lower threading dislocation density. Increasing the number of QWs eventually leads to performance degradation of devices grown on both substrates. Solar cells are demonstrated with peak external quantum efficiencies up to 60%, open circuit voltages up to 2.28 V, fill factors up to 80%, and conversion efficiencies up to 2.4% under 1 sun AM0 equivalent illumination. © *2013 AIP Publishing LLC*. [http://dx.doi.org/10.1063/1.4826483]

To significantly improve the efficiency of concentrating photovoltaic (CPV) systems the number of junctions in the multijunction solar cells (MJSCs) that generate power for those systems must be increased. Current state-of-the-art MJSCs with 3 or 4 junctions achieve greater than 40% power conversion efficiency under concentrations up to 1000 suns, but their top junctions are limited to bandgap energies below 2 eV.[1–3] Efficient utilization of higher energy photons requires an additional junction with a bandgap near 2.6 eV.[4,5] InGaN makes an ideal candidate for this additional junction because of its direct bandgap, high absorption coefficient, radiation resistance, and extensive development for use in high performance light-emitting diodes.[6–8] Although there have been several reports of InGaN/GaN photovoltaic devices, their performance tends to degrade at higher indium compositions and longer wavelengths.[9–12]

Growth of InGaN with indium composition exceeding 20% presents several challenges. Large piezoelectric polarization-induced electric fields hinder drift-based carrier collection in p-i-n devices, though this effect can be mitigated by heavy doping at the edges of the junction.[13] In addition, degradation of *c*-plane InGaN at high indium compositions begins after only a few nanometers of InGaN growth while hundreds of nanometers of InGaN are required for full absorption. As opposed to growing a single InGaN layer in a double heterostructure,[9] a multiple quantum well (MQW) active region design offers significant advantages in growth while not diminishing expected performance.[14] In particular, the MQW active region enables the growth of InGaN quantum wells (QWs) and GaN quantum barriers (QBs) under different growth conditions[15,16] so as to limit the formation of V-defects,[17] as discussed in more detail below.

There are two major reasons to decrease QB thickness in an MQW active region design. First, the presence of QBs increases the total thickness of the intrinsic active region, which must remain fully depleted to maintain an electric field and facilitate efficient drift transport. Unintentional background n-type doping (UID) on the order of $10^{16}\,cm^{-3}$, due to oxygen impurities, limits the depletion width of a one-sided p-UID junction to ~500 nm. It has also been demonstrated that QB thickness has a significant effect on carrier collection efficiency.[18] Carriers generated in the QWs must escape either by thermionic emission or tunneling processes, before being lost to recombination. Tunneling is the dominant escape mechanism from InGaN QWs near room temperature, and the tunneling rate increases strongly with decreasing barrier thickness.[18]

The need to decrease QB thickness must be balanced against the need to avoid V-defects, which form during low temperature *c*-plane GaN growth by metalorganic chemical vapor deposition (MOCVD). The V-defects nucleate on pre-existing threading dislocations (TDs) and then propagate outward on $10\bar{1}1$ planes, forming an inverted hexagonal pyramid-shaped pit.[17] V-defects act as non radiative recombination centers and leakage pathways, and they severely degrade the open-circuit voltage (V_{oc}) of InGaN solar cells.[19,20] A 2-step QB growth process must be employed to mitigate the propagation of V-defects through an InGaN/GaN MQW stack.[15,16] A low temperature GaN cap layer protects QW integrity, while the subsequent layer is grown at higher temperature and in H_2 to improve surface adatom mobility and effectively fill in the V-defects. To decrease the total QB thickness while maintaining a V-defect free MQW, the cap layer thickness and the second step growth temperature were concurrently optimized, resulting in a 2 nm cap and 4 nm total QB thickness, thinner than previously achieved.[15] In this letter, we demonstrate InGaN/GaN solar cells grown using this optimized MQW structure and compare devices grown on sapphire to those grown on native substrates.

MOCVD was used to grow InGaN/GaN MQW solar cells on co-loaded substrates consisting of half of a 50 mm double-side-polished (0001) sapphire wafer with a 2 μm n-GaN ($[Si] = 6 \times 10^{18}\,cm^{-3}$) template and a 5 mm × 5 mm piece of a hydride vapor phase epitaxy (HVPE) grown bulk

a)Electronic mail: ngyoung@engineering.ucsb.edu

(0001) GaN substrate from Furukawa Denshi Co., Ltd. The bulk (0001) GaN substrate had a threading dislocation density (TDD) of less than $3 \times 10^6\,cm^{-2}$, while the TDD of GaN grown on sapphire was at least 2 orders of magnitude higher.[21] The MOCVD growth consisted of a 2 μm Si-doped n-GaN ($[Si] = 6 \times 10^{18}\,cm^{-3}$) template layer followed by a 10 nm highly Si-doped n^+-GaN ($[Si] = 2 \times 10^{19}\,cm^{-3}$) layer. The intrinsic active region consisted of an undoped $In_{0.2}Ga_{0.8}N$/GaN MQW with 10 to 50 periods, 2.3 nm QWs for samples grown on sapphire, 3.0 nm QWs for samples grown on bulk (0001) GaN, and 4.0 nm QBs for all samples. The final QW was immediately followed by a 25 nm highly Mg-doped p^+-GaN ($[Mg] = 5 \times 10^{19}\,cm^{-3}$) layer, a 20 nm moderately Mg-doped p-GaN ($[Mg] = 2 \times 10^{19}\,cm^{-3}$) layer, and a 10 nm highly Mg-doped p^+-GaN contact layer ($[Mg] = 1 \times 10^{20}\,cm^{-3}$).

Following the MOCVD growth, the sample surfaces were characterized by atomic force microscopy (AFM) with a Digital Instruments Dimension 3000 AFM, the QW and QB thicknesses and indium composition were measured by x-ray diffraction (XRD) using a PANalytic MRD PRO diffractometer, and the layer thicknesses were confirmed by high angle annular dark field scanning transmission electron microscopy (HAADF-STEM). The absorption spectra of the samples were measured using a Shimadzu UV-3600 UV-VIS-NIR spectrophotometer coupled with an integrating sphere, as described elsewhere.[22] The samples were then processed into solar cells using standard contact lithography. Cl_2-based reactive ion etching was used to define 1 mm by 1 mm mesas. The p-contact scheme consisted of 30/300 nm Pd/Au electron-beam deposited grids on the top of each mesa with a grid spacing of 200 μm and a grid width of 5 μm, and the n-contact scheme consisted of 30/300 nm Al/Au electron-beam deposited rings around the base of each mesa. After fabrication, dark and illuminated current density versus voltage (J-V) measurements were taken using a Keithley 2632 source meter. An Oriel 300 W Xe lamp provided broadband illumination with an AM0 intensity of 1 sun, as determined by integration of the external quantum efficiency (EQE) spectra over the AM0 solar spectrum. EQE spectra were measured under monochromatic illumination using the same lamp with an Oriel 260 monochromator and were calibrated using a reference Si photodetector.

Figures 1(a) and 1(b) show the EQE and absorption spectra of solar cells with 10, 20, 30, and 50 QW periods grown concurrently on bulk (0001) GaN and sapphire, respectively. The bulk (0001) GaN devices increased in EQE across the spectrum with increasing QWs, and reached a peak EQE of 60% with 50 QWs. The sapphire devices, in contrast, showed a similar increase in EQE between 10 and 20 QWs, but diminishing improvement compared to the bulk (0001) GaN devices as the number of QWs increased above 20. In addition, the internal quantum efficiency (IQE), which can be extracted by taking the ratio of the EQE and absorption spectra, was significantly better for the bulk (0001) GaN devices with more than 20 QWs than for the sapphire devices with more than 20 QWs. IQE, which is a measure of carrier collection efficiency, is very sensitive to non-radiative recombination resulting from TDs and V-defects, so this trend is not surprising. Crossing of the absorption and EQE spectra near the absorption edge in Fig. 1(a) is not physical and likely resulted from on wafer wavelength variations between different measurement areas.

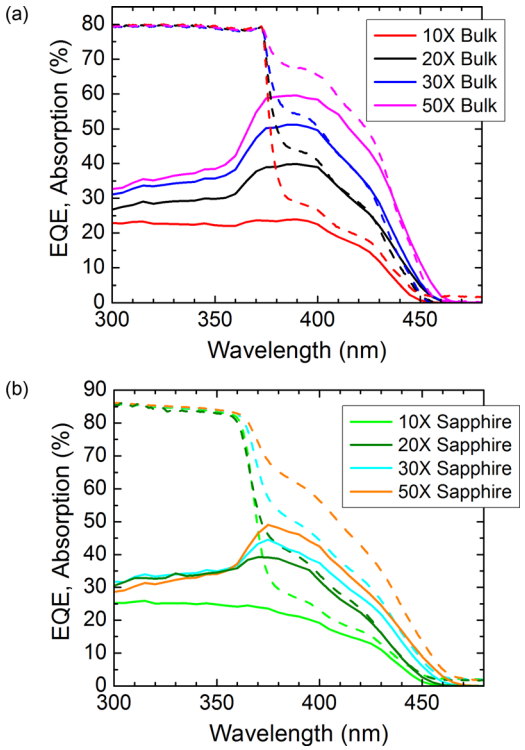

FIG. 1. EQE (solid lines) and absorption (dashed lines) measurements for samples with 10–50 QWs. Samples were grown on co-loaded (a) bulk (0001) GaN substrates and (b) sapphire substrates with 2 μm n-GaN templates.

Dark and illuminated J-V measurements for the solar cells on bulk (0001) GaN are presented in Fig. 2(a), while the corresponding measurements for solar cells on sapphire appear in Fig. 2(b). These thin barrier devices exhibited very high open circuit voltages (V_{oc}) as a whole, with values up to 2.28 V. Additionally, they demonstrated fill factors (FFs) up to 80%. The best performing device overall was the 30X MQW solar cell on bulk (0001) GaN, with a peak EQE of 51.2%, a V_{oc} of 2.26 V, a FF of 70.4%, a short circuit current density (J_{sc}) of 2.10 mA/cm^2, a maximum power density ($P_{d,max}$) of 3.33 mW/cm^2, and a conversion efficiency of 2.4% compared to the AM0 integrated power density of 1366.1 W/m^2.

The main difference between growth on non-native sapphire and native GaN substrates is the large difference in TDD in the epitaxial layers. Threading dislocations act as non-radiative recombination centers and leakage pathways in GaN-based devices;[23,24] therefore, we expected improved performance on bulk (0001) GaN substrates. A comparison of device performance for growth on sapphire and bulk (0001) GaN substrates can be seen in Figs. 3(a)–3(d), which show the dependence of V_{oc}, J_{sc}, FF, and $P_{d,max}$ on the number of QWs in the active region, respectively. Each of these values, with the exception of FF, clearly improved on bulk (0001) GaN substrates. On sapphire, the decrease of V_{oc} and FF and the relative drop of J_{sc} compared to bulk (0001) GaN are likely due to the propagation of V-defects through the MQW stack. AFM images have shown pits on sapphire samples starting with 20 QWs, and the size of the pits increases

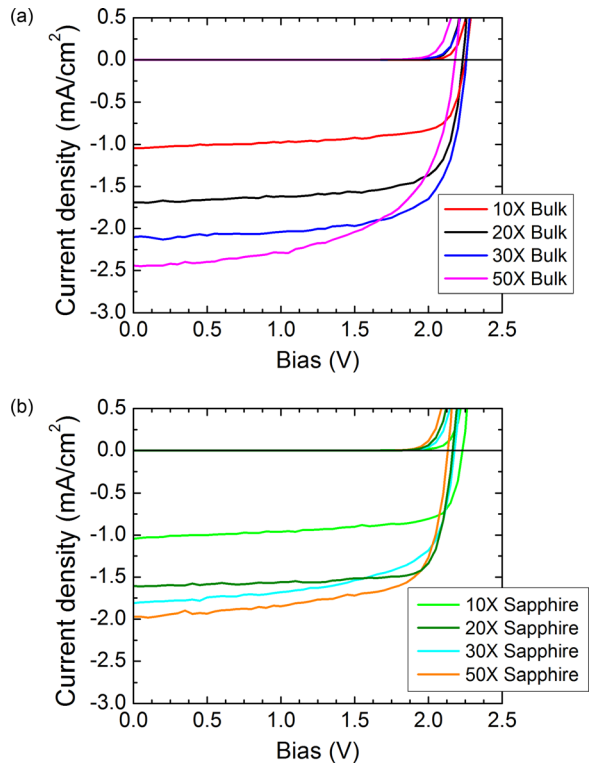

FIG. 2. *J-V* curves for samples with 10–50 QWs grown on coloaded (a) bulk (0001) GaN and (b) sapphire substrates.

monotonically with increasing QW number. Increasing the number of QWs promotes V-defect formation in this case,[17] despite growth conditions designed to prevent them.[15,16] All samples on bulk GaN, in contrast, were smooth and pit-free due to the low TDD. Nevertheless, some degradation still occurred between the 30 QW and 50 QW bulk (0001) GaN devices in the absence of V-defects, as indicated by the decrease seen in $P_{d,max}$ in Fig. 3(d).

Samples with 50 QWs on both sapphire and bulk (0001) GaN were investigated by HAADF-STEM to verify layer thicknesses and compare structural degradation mechanisms. Figure 4(a) shows a cross sectional image of the 50 QW sample on bulk (0001) GaN, with good structural quality through the entire stack, though there were some slight barrier width fluctuations. This contrasts with the image of the 50 QW sample on sapphire (Fig. 4(b)), which shows severe QW width fluctuations. In addition, it was noted that the QWs were 30% thicker (3.0 nm vs. 2.3 nm) on the bulk (0001) GaN substrate even though the samples were loaded during the same growth. The difference in InGaN growth rate without a change in GaN QB growth rate or a significant change in InGaN composition is not fully understood at this time and is a subject of further investigation. The resulting larger total thickness of InGaN on bulk (0001) GaN devices than on sapphire explains some of the difference in current and EQE due to higher absorption, but the IQE is also significantly better on bulk (0001) GaN (see Fig. 1), indicating the higher material quality on bulk (0001) GaN.

The HAADF-STEM images in Figs. 4(c) and 4(d) show one defect originating in the middle of the 50 QW stack and propagating in the [0001] growth direction. It is unlikely to have been associated with a preexisting TD since no TD was observed beneath the MQW, and the chance of finding a preexisting TD at this magnification with a TDD of less than $3 \times 10^6\,\mathrm{cm}^{-2}$ is very small. This defect is likely a TD initiated by a misfit dislocation generated within the MQW stack due to strain accumulation, which has been previously observed in InGaN QWs on bulk (0001) GaN.[25] This evidence of a structural degradation mechanism on bulk (0001) GaN that occurs without the presence of preexisting TDs would explain the drop in device performance between 30 QWs and 50 QWs.

The performance of the 30 QW device on bulk (0001) GaN is still far from that of an ideal InGaN solar cell with perfect growth quality, no defect generation, and enough

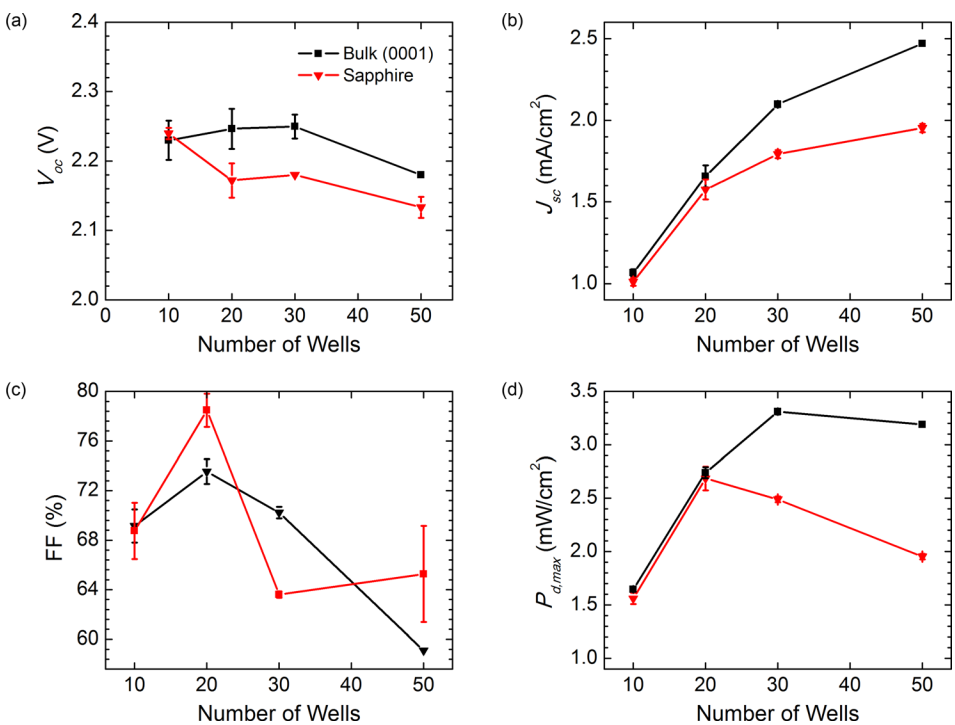

FIG. 3. Dependence of (a) open circuit voltage, (b) short-circuit current density, (c) fill factor, and (d) maximum power density on number of QWs for samples grown on coloaded bulk (0001) GaN and sapphire substrates.

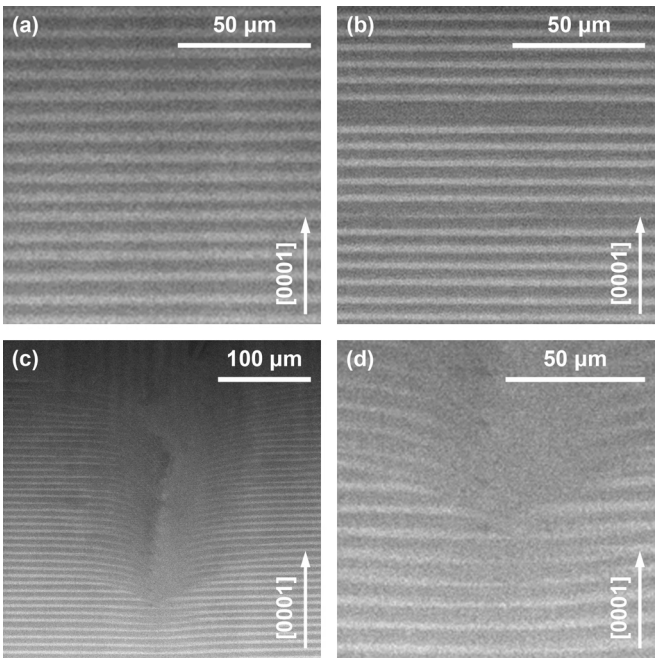

FIG. 4. HAADF-STEM images of partial MQW stacks for samples with 50 QWs grown on coloaded (a) bulk (0001) GaN and (b) sapphire substrates. Additionally, images of a defect in the (0001) bulk GaN 50 QW sample (c) at low magnification and (d) at higher magnification.

InGaN to absorb all of the incident light. Table I compares the actual values of J_{sc}, V_{oc}, FF, and $P_{d,max}$ from the 30 QW device to those of an ideal InGaN/GaN cell with the same bandgap. This ideal device is a p-i-n double heterostructure with 500 nm of $In_{0.2}Ga_{0.8}N$ in the active region for full absorption. Collection efficiency is assumed to be perfect so that EQE is 100% above the InGaN bandgap of 2.73 eV. Therefore, the ideal J_{sc} is calculated by integrating the AM0 solar irradiance spectrum normalized by photon energy over all wavelengths above the bandgap. Ideal V_{oc} is a function of the minimum effective bandgap-voltage offset $W_{oc,eff}$, defined as the difference between the solar cell's effective bandgap and V_{oc}.[26] The effective bandgap of 454 nm is estimated by extrapolating the linear shoulder of the EQE spectrum to the wavelength axis. In the ideal case where radiative recombination is the dominant recombination mechanism, $W_{oc,eff}$ is given by

$$W_{oc,eff} = \frac{kT}{q} \ln\left(\frac{qwBN_CN_V}{J_{ph}}\right), \quad (1)$$

where w is the active region thickness.[26] We use a value of 5×10^{-11} for B, the InGaN radiative recombination coefficient.[27] N_C and N_V are the conduction and valence band effective density of states for $In_{0.2}Ga_{0.8}N$,[28] respectively, and J_{ph} is the photogenerated current density, assumed to be equal to the ideal J_{sc}. Ideal FF can be approximated very closely by the following expression:

$$FF = \frac{v_{oc} - \ln(v_{oc} + 0.72)}{v_{oc} + 1}, \quad (2)$$

where v_{oc} is the normalized open circuit voltage, equal to ideal V_{oc} divided by nkT/q.[29] We assume the ideality factor n equals 2 since the active region is fully depleted in an ideal p-i-n structure.

TABLE I. Comparison of device parameters between values measured for the 30 QW InGaN/GaN solar cell on bulk (0001) GaN and values for an ideal InGaN-based solar cell with the same bandgap.

Parameter	Measured value	Theoretical value	Percent of ideal
J_{sc} (mA/cm^2)	2.10	6.23	33.7
$W_{oc,eff}$ (V)	0.47	0.388	78.9
V_{oc} (V)	2.26	2.343	96.5
FF (%)	70.4	89.5	78.7
$P_{d,max}$ (mW/cm^2)	3.33	13.06	25.5

It is clear from Table I that the J_{sc} shows the largest discrepancy compared to an ideal device and thus has the largest impact on the maximum output power, which is equal to $P_{d,max} = V_{oc} \times J_{sc} \times FF$. J_{sc} is limited mainly by the thickness of InGaN that can be grown before the onset of structural instabilities due to mismatch stresses, as seen in Fig. 4. Likewise, the FF can be improved significantly by limiting non-radiative recombination, while the V_{oc} is already very close to its theoretical value. One possible solution for preventing strain-related degradation is a strain-balanced InGaN/AlGaN MQW active region, though any solution will involve significant materials growth challenges.

In summary, we have demonstrated high performance InGaN/GaN MQW solar cells with thin barriers to promote efficient carrier transport. Growth on low TDD bulk (0001) GaN substrates provided improvements in performance compared to sapphire substrates, especially with an increasing number of QWs. Device degradation occurred as MQW thickness increased, with the onset being delayed on bulk (0001) GaN substrates. Our results indicate that V-defects form on preexisting TDs during MQW growth on sapphire, while new defects nucleate during MQW growth on bulk (0001) GaN. Our thin barrier solar cells exhibited EQEs up to 60%, V_{oc} as high as 2.28 V, FF up to 80%, and a maximum conversion efficiency of 2.4% under 1 sun AM0 equivalent illumination.

This work was supported by the Solid State Lighting and Energy Center (SSLEC). A portion of this work was performed in the UCSB nanofabrication facility, part of the NSF NNIN network (ECS-0335765), as well as the UCSB MRL, which was supported by the NSF MRSEC Program (DMR-1121053). The sapphire substrates and the trimethylindium metalorganic sources used for this study were provided by Namiki Precision Jewel and Sonata LLC, respectively.

[1]R. R. King, D. C. Law, K. M. Edmondson, C. M. Fetzer, G. S. Kinsey, H. Yoon, R. A. Sherif, and N. H. Karam, Appl. Phys. Lett. **90**, 183516 (2007).
[2]J. F. Geisz, D. J. Friedman, J. S. Ward, A. Duda, W. J. Olavarria, T. E. Moriarty, J. T. Kiehl, M. J. Romero, A. G. Norman, and K. M. Jones, Appl. Phys. Lett. **93**, 123505 (2008).
[3]M. Stan, D. Aiken, B. Cho, A. Cornfeld, V. Ley, P. Patel, P. Sharps, and T. Varghese, J. Cryst. Growth **312**, 1370–1374 (2010).
[4]N. G. Toledo and U. K. Mishra, J. Appl. Phys. **111**, 114505 (2012).
[5]N. G. Toledo, D. J. Friedman, R. M. Farrell, E. E. Perl, C. T. (Tony) Lin, J. E. Bowers, J. S. Speck, and U. K. Mishra, J. Appl. Phys. **111**, 054503 (2012).

[6]A. David and M. J. Grundmann, Appl. Phys. Lett. **97**, 033501 (2010).
[7]J. Wu, W. Walukiewicz, K. M. Yu, W. Shan, J. W. Ager, E. E. Haller, H. Lu, W. J. Schaff, W. K. Metzger, and S. Kurtz, J. Appl. Phys. **94**, 6477 (2003).
[8]M. R. Krames, O. B. Shchekin, R. Mueller-Mach, G. O. Mueller, L. Zhou, G. Harbers, and M. G. Craford, J. Disp. Technol. **3**, 160–175 (2007).
[9]C. J. Neufeld, N. G. Toledo, S. C. Cruz, M. Iza, S. P. DenBaars, and U. K. Mishra, Appl. Phys. Lett. **93**, 143502 (2008).
[10]X. Chen, K. D. Matthews, D. Hao, W. J. Schaff, and L. F. Eastman, Phys. Status Solidi A **205**, 1103–1105 (2008).
[11]R. M. Farrell, C. J. Neufeld, S. C. Cruz, J. R. Lang, M. Iza, S. Keller, S. Nakamura, S. P. DenBaars, U. K. Mishra, and J. S. Speck, Appl. Phys. Lett. **98**, 201107 (2011).
[12]R. Dahal, B. Pantha, J. Li, J. Y. Lin, and H. X. Jiang, Appl. Phys. Lett. **94**, 063505 (2009).
[13]C. J. Neufeld, S. C. Cruz, R. M. Farrell, M. Iza, J. R. Lang, S. Keller, S. Nakamura, S. P. DenBaars, J. S. Speck, and U. K. Mishra, Appl. Phys. Lett. **98**, 243507 (2011).
[14]K. W. J. Barnham, I. Ballard, J. P. Connolly, N. J. Ekins-Daukes, B. G. Kluftinger, J. Nelson, and C. Rohr, Physica E **14**, 27–36 (2002).
[15]Y. L. Hu, R. M. Farrell, C. J. Neufeld, M. Iza, S. C. Cruz, N. Pfaff, D. Simeonov, S. Keller, S. Nakamura, S. P. DenBaars, U. K. Mishra, and J. S. Speck, Appl. Phys. Lett. **100**, 161101 (2012).
[16]S. M. Ting, J. C. Ramer, D. I. Florescu, V. N. Merai, B. E. Albert, A. Parekh, D. S. Lee, D. Lu, D. V. Christini, L. Liu, and E. A. Armour, J. Appl. Phys. **94**, 1461 (2003).
[17]X. H. Wu, C. R. Elsass, A. Abare, M. Mack, S. Keller, P. M. Petroff, S. P. DenBaars, J. S. Speck, and S. J. Rosner, Appl. Phys. Lett. **72**, 692 (1998).
[18]J. R. Lang, N. G. Young, R. M. Farrell, Y. R. Wu, and J. S. Speck, Appl. Phys. Lett. **101**, 181105 (2012).
[19]L. C. Le, D. G. Zhao, D. S. Jiang, L. Li, L. L. Wu, P. Chen, Z. S. Liu, Z. C. Li, Y. M. Fan, J. J. Zhu, H. Wang, S. M. Zhang, and H. Yang, Appl. Phys. Lett. **101**, 252110 (2012).
[20]M. Mori, S. Kondo, S. Yamamoto, T. Nakao, T. Fujii, M. Iwaya, T. Takeuchi, S. Kamiyama, I. Akasaki, and H. Amano, Appl. Phys. Express **5**, 082301 (2012).
[21]X. H. Wu, L. M. Brown, D. Kapolnek, S. Keller, B. Keller, S. P. Denbaars, and J. S. Speck, J. Appl. Phys. **80**, 3228 (1996).
[22]E. Matioli, C. Neufeld, M. Iza, S. C. Cruz, A. A. Al-Heji, X. Chen, R. M. Farrell, S. Keller, S. DenBaars, U. Mishra, S. Nakamura, J. Speck, and C. Weisbuch, Appl. Phys. Lett. **98**, 021102 (2011).
[23]Q. Dai, M. F. Schubert, M. H. Kim, J. K. Kim, E. F. Schubert, D. D. Koleske, M. H. Crawford, S. R. Lee, A. J. Fischer, G. Thaler, and M. A. Banas, Appl. Phys. Lett. **94**, 111109 (2009).
[24]P. Kozodoy, J. P. Ibbetson, H. Marchand, P. T. Fini, S. Keller, J. S. Speck, S. P. DenBaars, and U. K. Mishra, Appl. Phys. Lett. **73**, 975 (1998).
[25]M. Zhu, S. You, T. Detchprohm, T. Paskova, E. A. Preble, and C. Wetzel, Phys. Status Solidi A **207**, 1305–1308 (2010).
[26]R. R. King, D. Bhusari, A. Boca, D. Larrabee, X.-Q. Liu, W. Hong, C. M. Fetzer, D. C. Law, and N. H. Karam, Prog. Photovolt: Res. Appl. **19**, 797–812 (2011).
[27]X. Li, S. Okur, F. Zhang, V. Avrutin, U. Ozgur, H. Morkoc, S. M. Hong, S. H. Yen, T. C. Hsu, and A. Matulionis, J. Appl. Phys. **111**, 063112 (2012).
[28]E. F. Schubert, *Light Emitting Diodes*, 2nd ed. (Cambridge University Press, 2006).
[29]M. Green, Sol. Cells **7**, 337–340 (1982).